

# Localization effects from local phase shifts in the modulation of waveguide arrays

KONRAD TSCHERNIG,<sup>1,\*</sup> ARMANDO PEREZ-LEIJA,<sup>1</sup> AND KURT BUSCH<sup>2,3</sup>

<sup>1</sup>CREOL, The College of Optics and Photonics, University of Central Florida, Orlando, FL 32816, USA

<sup>2</sup>Max-Born-Institut, 12489 Berlin, Germany

<sup>3</sup>Humboldt-Universität zu Berlin, Institut für Physik, AG Theoretische Optik & Photonik, 12489 Berlin, Germany

\*konrad.tschernig@knights.ucf.edu

**Abstract:** Artificial gauge fields enable the intriguing possibility to manipulate the propagation of light as if it were under the influence of a magnetic field even though photons possess no intrinsic electric charge. Typically, such fields are engineered via periodic modulations of photonic lattices such that the effective coupling coefficients after one period become complex-valued. In this work, we investigate the possibility to introduce randomness into artificial gauge fields by applying local random phase shifts in the modulation of lattices of optical waveguides. We first study the elemental unit consisting of two coupled single-mode waveguides and determine the effective complex-valued coupling coefficient after one period of the modulation as a function of the phase shift, the modulation amplitude and the modulation frequency. Thereby we identify the regime where varying the modulation phase yields sufficiently large changes of the effective coupling coefficient to induce Anderson localization. Using these results, we demonstrate numerically the onset of Anderson localization in 1D- and 2D-lattices of  $x$ -, and helically-modulated waveguides via randomly choosing the modulation phases of the individual waveguides. Besides further fundamental investigations of wave propagation in the presence of random gauge fields, our findings enable the engineering of the coupling coefficients without changing the footprint of the overall lattice. As a proof of concept, we demonstrate how to engineer out-of-phase modulated lattices which exhibit dynamic localization and defect-free surface states. Therefore, we anticipate that the modulation phase will play an important role in the judicious design of functional waveguide lattices.

© 2023 Optica Publishing Group

## 1. Introduction

Anderson localization [1] is the phenomenon of wave localization via multiple scattering in disordered systems. More precisely, for sufficiently strong disorder, interference processes change the physical nature of waves from propagating to localized so that Anderson localization represents a universal phenomenon and occurs in numerous wave systems [2, 3], including optics, acoustics, and crystals. Historically, Anderson localization has first been studied in electronic systems where additional effects such as electron-electron interaction and the application of magnetic fields modify the characteristics of the Anderson transition, thereby providing a rich field for both fundamental research (e.g. field theories) and exciting applications (e.g. quantum-Hall-effect based devices) [4]. In fact, Anderson localization has also been demonstrated in classical wave systems such as acoustics [5, 6], optics [7–10], and in crystals [4]. For instance, arrays of coupled optical waveguides [11], ring resonators [12] or optical cavities [13] are described via tight-binding models where the on-site (diagonal) 'potentials' are given by the individual waveguides' propagation constants or resonance frequencies of the individual resonators/cavities. By the same token, the (off-diagonal) 'hopping' elements between sites are determined by the modal overlap of the waveguide modes or the resonator/cavity modes. For instance, in arrays of coupled waveguides both on- and off-diagonal disorder can be readily induced and controlled [10] by manipulating the effective refractive index of the individual waveguides [7] and the distance between them [8].

Nonetheless, the aforementioned richness of electronic systems appears to be out of reach for optical systems, since electron-electron interaction and the effects of magnetic fields generally require the presence of electric charges. However, there exists an intriguing possibility to modify the flow of light via artificial gauge fields [14]. Such fields can be induced via periodic modulation of photonic lattice structures, for example by changing the transverse positions of a waveguide array in a periodic fashion [15]. Then, periodic modulations in the waveguide positions induce complex-valued off-diagonal coupling parameters ('hopping' elements), which are directly associated to an artificial gauge field that acts on the propagation of light (see section 2). Notably, this effect occurs despite the fact that photons possess no intrinsic electric charge. Such artificial gauge fields have been exploited to implement, for example, photonic Floquet topological insulators [16] and to guide light in novel fashions on different optical platforms [17–24].

With a view on Anderson localization, the need to control the gauge field locally emerges and has been the subject of several recent studies in the context of resonator lattices [19, 25]. In this work, we study theoretically and numerically the possibility of generating locally random gauge fields in modulated waveguide arrays. We achieve this by introducing random phase shifts (modulation phases) along the propagation direction into the modulation of the waveguide positions in regular 1D- and 2D-lattices. When the waveguides are modulated in a helical fashion or along the lattice axis, we find

that disorder in the modulation phases translates directly into disorder in the effective coupling coefficients. Beyond Anderson localization our findings on the modulation phase open up a new pathway to engineer the coupling behavior in photonic lattices. Specifically, our approach allows for increasing and decreasing the coupling as desired without changing the average distance between the waveguides and, thus, without affecting the overall footprint of the photonic lattice. As a proof of concept, we obtain and tune dynamic localization effects [26, 27] by choosing the modulation phases judiciously.

## 2. Artificial gauge fields from periodic modulations

Let us first elaborate on the origin of artificial gauge fields via periodic modulation of waveguide arrays. To set the stage, we begin with the Helmholtz equation in paraxial approximation [28] for waves propagating in  $z$ -direction

$$i\partial_z\psi(x, y, z) = \left[ -\frac{1}{2k_0} (\partial_x^2 + \partial_y^2) + V \right] \psi(x, y, z), \quad (1)$$

where  $k_0 = 2\pi/\lambda$  is the wave number,  $\psi(x, y, z)$  is the slowly-varying field envelope,  $x, y$  the transverse coordinates,  $z$  the propagation distance and the potential  $V$  encodes the refractive index profile. We start by considering a lattice of  $N$  straight waveguides, such that  $V = V(x, y) = \sum_{n=1}^N V_0(x-x_n, y-y_n)$  and  $V_0(x, y)$  is the refractive index profile of a single straight waveguide centered at the origin  $(x, y) = (0, 0)$ , and  $(x_n, y_n)$  is the transverse position of the  $n$ 'th waveguide. To introduce periodic modulations, we shift the waveguide centers according to  $(x_n, y_n) \rightarrow (x_n + R_x \cos(\omega z), y_n + R_y \sin(\omega z))$ , where  $R_{x/y}$  are the modulation radii and  $\omega$  is the modulation frequency along the propagation direction. Evidently, this introduces a  $z$ -dependence into the potential  $V(x, y) \rightarrow V(x, y, z) = \sum_{n=1}^N V_0(x - R_x \cos(\omega z) - x_n, y - R_y \sin(\omega z) - y_n)$ . However, by transforming into the co-rotating reference frame  $(x', y', z') = (x - R_x \cos(\omega z), y - R_y \sin(\omega z), z)$  we can eliminate the  $z$ -dependence in the potential and, instead, acquire an artificial gauge in the new coordinate system

$$i\partial_{z'}\psi(x', y', z') = \left[ -\frac{1}{2k_0} (\vec{\nabla} - i\vec{A}(z'))^2 + V(x', y') + \Phi(z') \right] \psi(x', y', z'), \quad (2)$$

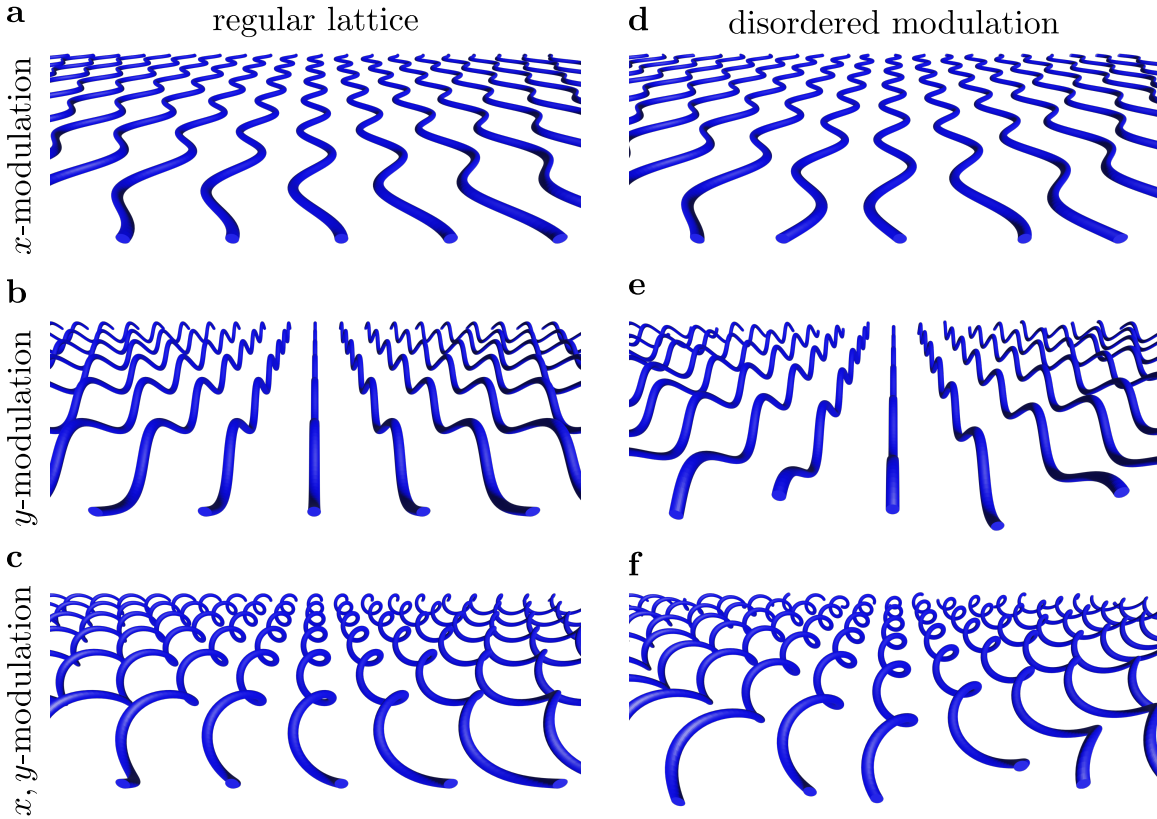


Fig. 1. **Modulated waveguide arrays exhibiting artificial gauge fields.** **Panels a-c:** Regular lattices of waveguides subjected to  $x$ -,  $y$ - and helical modulation, respectively. **Panels d-f:** Illustration of random phase-shifts in the modulation, and thereby, disorder in the artificial gauge field.

where  $\vec{\nabla} = (\partial_{x'}, \partial_{y'})^T$  and  $\vec{A}(z') = k_0\omega(R_x \sin(\omega z'), -R_y \cos(\omega z'))^T$  is the artificial gauge field. Additionally, we acquire the  $z'$ -dependent term  $\Phi(z') = -\frac{1}{2}k_0\omega^2(R_x^2 \sin^2(\omega z') + R_y^2 \cos^2(\omega z'))$ , which commutes with all the other terms on the right hand side of Eq. (2), since it is independent of the transverse coordinates. Therefore, it will only contribute a global phase factor  $\exp\left(-i \int_0^{z'} \Phi(z'') dz''\right)$  to the solution  $\psi(x', y', z')$  and will not contribute to the output light intensities  $|\psi(x', y', z')|^2$ . Crucially, the periodically modulated waveguide array is now equivalent to a lattice of straight waveguides in which the light is subjected to an artificial external magnetic field  $\vec{B} = \vec{\nabla} \times \vec{A}$ . To further elucidate the impact of the artificial gauge field on the evolution dynamics, we arrange the waveguides in a regular lattice, see Fig. (1-a,b,c) along the  $x$ -axis,  $(x_n, y_n) \rightarrow (na, 0)$ , where  $a$  is the lattice constant, and perform a Peierls' substitution [29] to obtain the tight-binding equation

$$i\partial_z\psi_m = \sum_{n=1}^N H_{m,n}(z)\psi_n. \quad (3)$$

Here  $\psi_m$  is the amplitude of the guided mode of the  $m$ 'th waveguide and  $H_{m,n}(z)$  denotes the  $z$ -dependent tight-binding Hamiltonian describing the hopping of the light-amplitudes among the lattice sites. Note that we have dropped the "prime" on the coordinates for the sake of brevity. In particular we assume the waveguides to be identical, such that  $H_{n,n} = \beta = 0$ , and only allow nearest neighbor coupling  $H_{n,n+1}(z) = \kappa e^{i\phi(z)} = H_{n+1,n}^*(z)$  ( $H_{n,m}(z) = 0$  otherwise). Here,  $\kappa$  is the real and positive coupling coefficient between nearest neighbors and  $\phi(z) = \vec{A}(z) \cdot \vec{a} = ak_0R_x\omega \sin(\omega z)$  is the effective artificial gauge field and  $\vec{a} = (a, 0)^T$  is the lattice vector. In first-order approximation we can write the effective  $z$ -independent Hamiltonian  $\hat{H}_{\text{eff}}$ , which governs the evolution over one period  $Z$ , as  $\hat{H}_{\text{eff}} = 1/Z \int_0^Z \hat{H}(z) dz$  [30], which is the average over one period. Thus, we find the effective coupling coefficient

$$\kappa_{\text{eff}} = \frac{\kappa}{Z} \int_0^Z e^{iak_0R_x\omega \sin(\omega z)} dz = \kappa J_0(ak_0R_x\omega), \quad (4)$$

which is a well-known result [30], and implies that the effective coupling strength between the waveguides can be controlled by changing the nearest-neighbor distance, wave length, modulation radius and frequency. In what follows we introduce and study an additional degree of freedom in the form of a relative phase shift in the modulation of the waveguides.

### 3. Random artificial gauge fields

We now study the effects of adding local random phase shifts  $\varphi_n$  to the periodic modulation of the waveguide positions, as we show in Fig. (1-d,e,f). Therefore, we consider the  $z$ -dependent potential of the form  $V(x, y, z) = \sum_{n=1}^N V_0(x - R_x \cos(\omega z + \varphi_n) - x_n, y - R_y \sin(\omega z + \varphi_n) - y_n)$ . In other words, each waveguide performs the same transverse movement as before but is now displaced along the  $z$ -direction by the amount  $z_n = \varphi_n/\omega$ . Clearly, there is no single reference frame within which the potential is rendered completely  $z$ -independent. Then the question arises immediately, whether a gauge field can even exist under such circumstances. We answer this positively and to see that, we first consider a pair of waveguides  $N = 2$  as we show in Fig. (2). Without loss of generality we choose the first waveguide as the reference and set  $\varphi_1 = 0$  and relabel  $\varphi_2 \rightarrow \varphi$ . Following the recipe outlined above, we transform

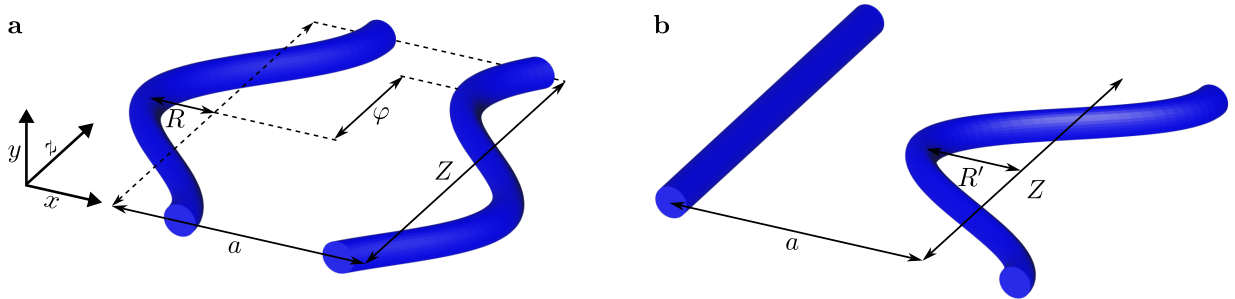


Fig. 2. **Two modulated coupled waveguides.** **Panel a:** In the laboratory frame of reference both waveguides are modulated with period  $Z$ , radius  $R$  and relative phase shift  $\varphi$ . Note, the center points of the modulation are separated by the distance  $a$  (lattice constant). **Panel b:** When transformed into the rest-frame of the first waveguide the system is equivalent to a single straight waveguide coupled to a modulated waveguide with the effective modulation radius  $R' = 2R \sin(\varphi/2)$  subjected to an artificial gauge field.

into the co-rotating frame of reference of the first waveguide  $(x', y', z') = (x - R_x \cos(\omega z), y - R_y \sin(\omega z), z - \frac{\varphi}{2\omega})$  and arrive at the transformed potential  $V(x', y', z') = V_0(x', y') + V_0(x' - a + R'_x \sin(\omega z'), y' - R'_y \cos(\omega z'))$ , with the effective modulation radii  $R'_{x/y} = 2R_{x/y} \sin(\varphi/2)$  and observe that the  $z'$ -dependence of the second waveguide potential remains. To take the movement of the second waveguide into account, we model the real-valued coupling coefficient  $\kappa$  as an exponentially decaying function of their distance  $d = |\vec{a}|$ ,  $\kappa(z') = \kappa_0 e^{-\xi |\vec{a}(z')|} e^{i\phi(z')}$ , where  $\kappa_0$  and  $\xi$  are real and positive fit-parameters. Note that we obtain the same vector potential as before except for a phase shift  $\vec{A}(z', \varphi) = k_0 \omega (R_x \sin(\omega z' + \varphi/2), -R_y \cos(\omega z' + \varphi/2))$ . Additionally, the displacement vector  $\vec{a}(z', \varphi) = (2R_x \sin(\varphi/2) \sin(\omega z') - a, 2R_y \sin(\varphi/2) \cos(\omega z'))^T$  between the waveguides is now a function of  $z'$  and  $\varphi$ . Thus, in first-order approximation, we expect from our theory that the effective coupling coefficient over one period to be a function of the modulation phase

$$\kappa_{\text{eff}}(\varphi) = \frac{\kappa_0}{Z} \int_0^Z e^{-\xi |\vec{a}(z', \varphi)|} e^{i\vec{A}(z', \varphi) \cdot \vec{a}(z', \varphi)} dz'. \quad (5)$$

Let us now verify these theoretical considerations. Our goal is to obtain the effective (tight-binding) coupling coefficient after one period of the modulation and to study its dependence on the modulation phase. To this end, we employ the beam propagation method (BPM) to solve the paraxial equation, Eq. (1), numerically. From the BPM simulations we obtain the evolution operator  $\hat{U}(Z)$  and extract the effective coupling from it. First, we setup two waveguides at distance  $a$  and modulate their positions as described above. Next, we launch the guided mode  $|\psi_n(0)\rangle$  of each waveguide,  $n = 1, 2$ , to obtain the corresponding output distribution  $|\psi_n(Z)\rangle$  after one period of the modulation. Evidently, the input and output fields are related by  $|\psi_n(Z)\rangle = \hat{U}(Z) |\psi_n(0)\rangle$ , which enables us to find the matrix elements of the propagation operator via

$$U_{m,n}(Z) := \langle \psi_m(0) | \hat{U}(Z) | \psi_n(0) \rangle = \langle \psi_m(0) | \psi_n(Z) \rangle, \quad (6)$$

where the inner product is defined as  $\langle \psi | \phi \rangle = \sum_{p,q} \phi_{p,q} \psi_{p,q}^*$  and  $\psi_{p,q}$  is the field amplitude on the (numerical) discretization point with indices  $p, q$ . To find the effective coupling coefficient  $\kappa_{\text{eff}} = \kappa e^{i\phi}$  we assume that the effective Hamiltonian acquires the form

$$\hat{H}_{\text{eff}} = \begin{pmatrix} 0 & \kappa e^{i\phi} \\ \kappa e^{-i\phi} & 0 \end{pmatrix}. \quad (7)$$

By identifying  $\hat{U}(Z) = e^{iZ\hat{H}}$  and after some algebra we find  $\kappa = \frac{\omega}{2\pi} \arctan(|\lambda_+ + \lambda_-|/|\lambda_+ - \lambda_-|)$  and  $\phi = \arccos(1 - |\vec{v}_+^T \cdot \vec{v}_-|^2)/2$ , where  $\lambda_{\pm} (\vec{v}_{\pm})$  are the eigenvalues (eigenvectors) of  $\hat{U}(Z)$ .

We now perform parameter scans over the modulation radius  $R \in [0, R_{\text{max}}]$ , the modulation frequency  $\omega \in [\pi/cm, 10\pi/cm]$  and the modulation phase  $\phi \in [0, \pi]$  and obtain the corresponding effective coupling coefficient  $\kappa_{\text{eff}}$  for three different cases of modulation:  $x$ - ( $R_x = R, R_y = 0$ ),  $y$ - ( $R_x = 0, R_y = R$ ) and helical modulation ( $R_x = R = R_y$ ).

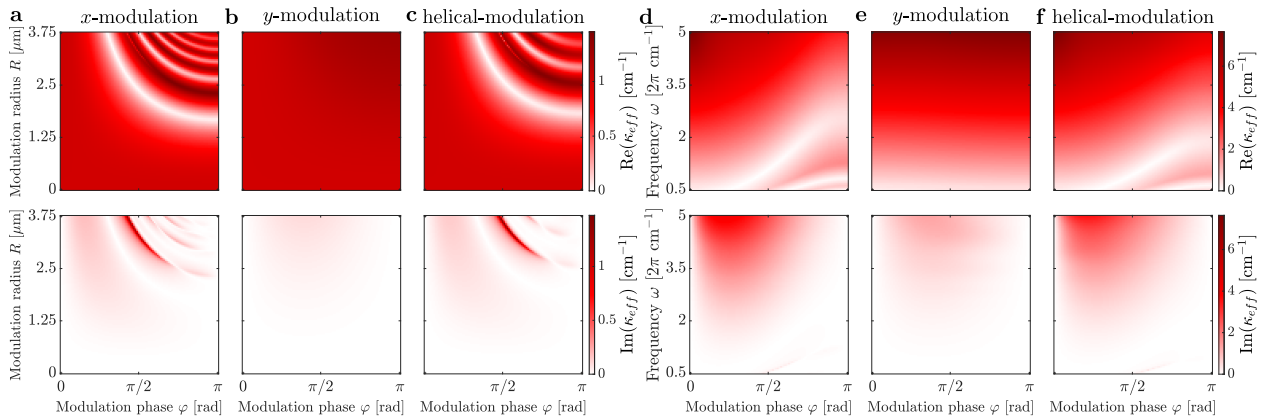


**Fig. 3. Parameter scans over the modulation phase  $\varphi$  versus modulation radius  $R$  (a-c) and versus the modulation frequency  $\omega$  (d-f).** For each parameter pair we performed BPM simulations over one period  $Z = 2\pi/\omega$  (wavelength  $\lambda = 450$  nm, distance between modulation centers  $a = 10 \mu\text{m}$ , waveguide diameter  $d = 2.5 \mu\text{m}$ , relative refractive index contrast  $\Delta n_0 = 1.55 \cdot 10^{-3}$ ) of the waveguide dimer and extracted the effective coupling coefficient  $\kappa_{\text{eff}}$ , for **a, d**  $x$ -modulation, **b, e**  $y$ -modulation and **c, f** helical modulation. The top (bottom) panels show the real (imaginary) part of  $\kappa_{\text{eff}}$ . In the scans over the radii we have chosen  $\omega = 2\pi/cm$  and in the scans over the frequencies we chose  $R = 2.5\mu\text{m}$ .

Note, that we choose  $R_{\max} = (a - d)/2$ , where  $d$  is the waveguide diameter, so that the waveguides do not overlap during any point of the propagation. Furthermore, we avoid too small modulation periods to minimise bending losses. Our results are summarized in Figs. (3). First of all, we observe that in the case of  $y$ -modulation, Fig. (3-b,e), that the coupling between the waveguides is almost completely independent of the modulation radius and phase. Thus, we can expect that random disorder in the modulation phase will not be able to induce Anderson localization under  $y$ -modulation for any modulation radius  $R$ . On the other hand, for  $x$ - and helical modulation, we find a significant change of the coupling when  $R \gtrsim 2\mu\text{m}$  over the whole range of the modulation phase and frequency.

#### 4. Anderson localization from locally disordered gauge fields

Now we are in the position to study Anderson localization due to disorder in the modulation phase. In order to observe Anderson localization, we require sufficiently strong disorder in the coupling coefficients. As we have shown in the previous section, we expect to achieve this using  $x$ - and helical modulation with a modulation radius  $R = 2.5\mu\text{m}$  and a modulation frequency of  $\omega = 2\pi/\text{cm}$ . Let us first study the 1D-case of linear arrays of waveguides and then the case of 2D lattices.

We now launch light into the center of a  $N = 40$  waveguide array and let it propagate for  $z = 10$  cm and take the average over an ensemble of  $N_{\text{ens}} = 50$  instances of the randomly chosen modulation phases  $\varphi_n \in [0, 2\pi]$ . In Fig. (4-a,b,c), we show the evolution of the ensemble-averaged intensity in the disordered lattices. Note, we show the integrated intensity  $I(x, z) = \int |\psi(x, y, z)|^2 dy$  and also chose to plot  $\sqrt{I}$  in order to improve the visibility of small intensities. We observe localization of the light in the  $x$ - and helical modulation, while the light exhibits the usual discrete diffraction behaviour in the case of  $y$ -modulation, compare with Fig. (4-g,h) where we show the discrete diffraction pattern in a lattice of straight waveguides without disorder. To further corroborate our findings we show the output intensity as a logarithmic plot in Fig. (4-d,e,f). Here, we observe a triangular shape of the intensity distribution which is characteristic of Anderson localization and indicates the exponential decay of the intensity in the transverse direction from the initial excitation site, which is completely absent for  $y$ -modulation.

In the light of these findings we now turn our attention to disordered 2D lattices. For our numerical experiments we set up a square lattice of  $21 \times 21$  waveguides. We choose  $a = 10 \mu\text{m}$ ,  $\omega = 2\pi/\text{cm}$  and  $R = 2.5 \mu\text{m}$ , facilitating sufficient disorder in the coupling when the modulation phases are chosen randomly. Due to the symmetry of this setup, we only need to consider the cases of helical- and  $x$ -modulation since  $y$ -modulation is now equivalent to  $x$ -modulation, apart from a trivial  $90^\circ$  rotation around the  $z$ -axis. We launch light in the center of the square lattice and obtain the average of the intensity evolution over  $N_{\text{ens}} = 20$  instances of the modulation disorder over a propagation distance of  $z = 10$  cm. In Fig. (5) we depict the corresponding results. As can be seen in Fig. (5-a-e), under helical modulation, the light experiences Anderson localization in both  $x$ - and  $y$ -direction. This is rather unsurprising, since in 2D the helical modulation is indistinguishable from  $x$ -modulation in the 1D case. The more interesting case is the  $x$ -modulation, as seen in Fig. (5-f-j). From the previous 1D-results one might expect to see the simultaneous existence of Anderson localization (in  $x$ -direction) and discrete diffraction (in  $y$ -direction). While we indeed observe Anderson localization in the modulation direction, we encounter a completely different behaviour in the perpendicular direction. Firstly,

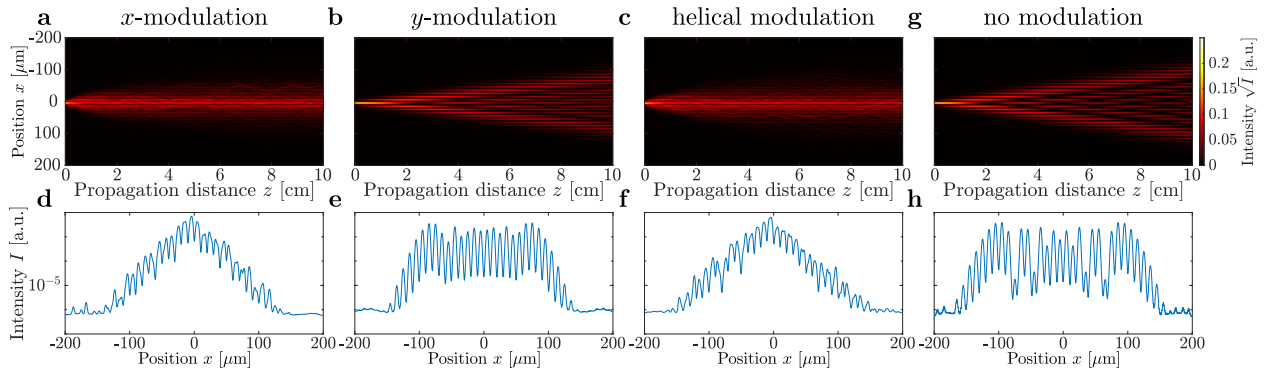


Fig. 4. **Anderson localization from random modulation phases.** **a-c** Intensity evolution averaged over 50 instances of the randomly chosen modulation phases  $\varphi_n \in [0, 2\pi]$  for  $x$ -,  $y$ -, and helical modulation respectively. In all cases we set the corresponding modulation radius to  $R = 2.5\mu\text{m}$ . **d-f** Logarithm of the output intensity distributions. In the case of  $x$ - and helical modulation, we observe the signatures of Anderson localization in the exponential decay of the averaged intensity along the transverse direction  $x$ . For  $y$ -modulation, the disorder in the modulation phases does not introduce sufficiently strong disorder in the effective coupling coefficient to localize the light. **g-h** For comparison we show the evolution of a single-site excitation in a lattice of straight waveguides without any modulation or disorder.

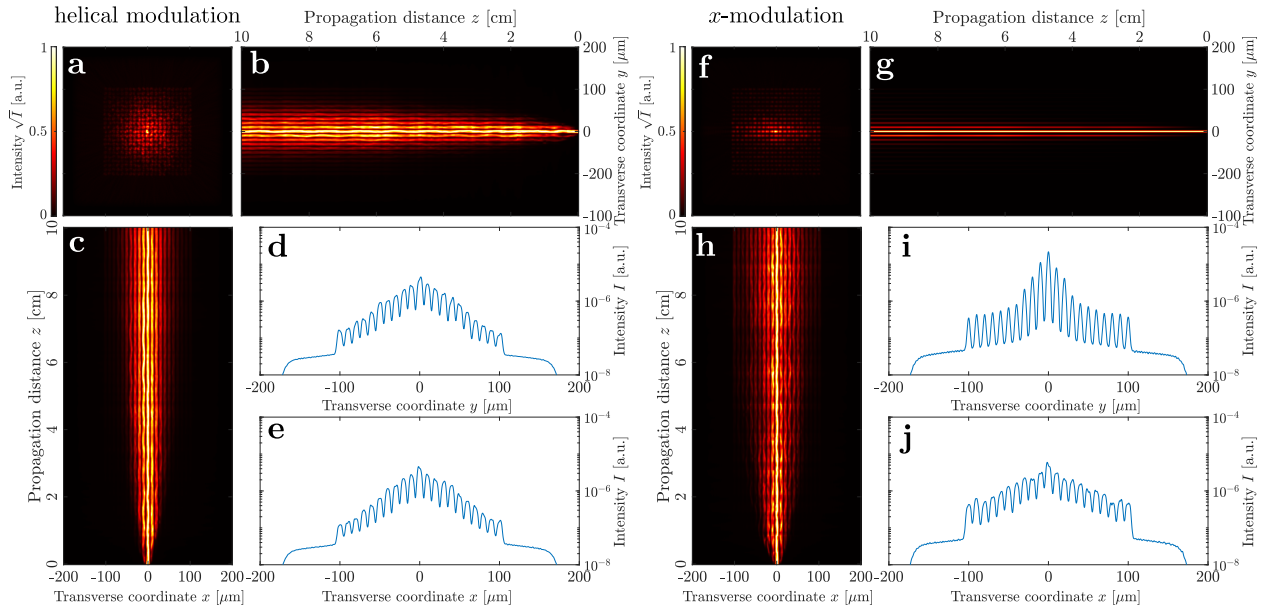


Fig. 5. **2D Anderson localization from random modulation phases.** We show the ensemble-averaged intensity evolution in random-out-of-phase modulated 2D arrays of waveguides (square  $21 \times 21$  lattice) under (a-e) helical modulation and (f-j)  $x$ -modulation. a, f Output intensity b, g Intensity along propagation direction (integrated over  $x$ -direction) c, h Intensity along propagation (integrated over  $y$ -direction) d, e, i, j Logarithmic plot of the output intensity along the  $x$ - ( $y$ -) direction.

we would like to note the logarithmic plot of the output intensities in Fig. (5-i), which suggests an almost Gaussian distribution of the light rather than the exponentially localized ones in Fig. (5-d,e,j). Further, it is worth to appreciate the degree of slowdown that the light experiences in its spreading in  $y$ -direction when compared to the  $x$ -direction. These observations raise the first question, of why we do not observe discrete diffraction in  $y$ -direction? To answer this, it is important to realize that the intensity distributions shown in Fig. (5-g,i) are averaged not only over the ensemble but also over the  $x$ -coordinate. Thus, even before ensemble-averaging, we observe an incoherent superposition of diffraction processes that “began” at random positions along the  $x$ - and  $z$ -axis, thereby smoothing out the typical 1D-interference pattern shown in Fig. (4-b,g). Furthermore, in this 2D setup we can expect that significant coupling between next-nearest neighbors in the diagonal directions occurs, thereby further inhibiting a clean diffraction pattern. While these explanations seem rather intuitive, they do not explain the significant narrowing of the intensity distribution and it is yet unclear how to properly characterize the process in  $y$ -direction. We conjecture that this behaviour constitutes either the early onset of Anderson localization (exhibiting a much larger localization length in  $y$  than in  $x$ ) or a slow diffusion-like process of light or maybe a mixture of the two. This question certainly merits further investigations.

## 5. Dynamic localization from out-of-phase modulation

Until now we have utilized the modulation phase to introduce disorder in the local effective gauge fields and the resulting effective coupling coefficients in waveguide lattices. Another intriguing possibility is the judicious design of the local effective gauge field in order to achieve a desired transformation. As a proof of concept we demonstrate how to obtain lattices exhibiting dynamic localization (DL), a well-known effect that occurs in periodically modulated lattices [26, 27]. For example, for in-phase modulated arrays, DL is achieved at the roots of the  $J_0$  Bessel-function in Eq. (4) and this constitutes the most prevalent case that has been studied in the past [27, 31]. Notably, Huang et. al [32] report a DL effect due to the  $\pi$ -out-of-phase refractive index modulation in sub-wavelength-scale light-guiding structures. Here we demonstrate numerically how to obtain DL in  $\varphi$ -out-of-phase modulated structures.

To obtain DL, the effective coupling coefficient after one period must vanish. This means that a single-site excitation launched in waveguide  $n$  will return to the same waveguide after one period, although the wavefunction may spread out to some extent in between. Thus we need to find the modulation parameters such that the effective coupling vanishes or is minimized. As an example we choose  $x$ -modulation,  $R = 2.5 \mu\text{m}$ ,  $a = 10 \mu\text{m}$  and  $\omega = 2\pi/\text{cm}$ . Using Fig. (3-a) we find that the coupling is minimized for a modulation phase of  $\varphi_d = 84.295^\circ$ . Now we need a 1D lattice of waveguides in which each nearest-neighbor pair of waveguides exhibits this relative modulation phase. This is achieved by choosing  $\varphi_{2n} = 0$  and  $\varphi_{2n+1} = \varphi_d$ , in other words, by alternating the modulation phase along the waveguide array. In Fig. (6-a) we show the resulting lattice structure and the evolution of a single-site excitation of the central waveguide  $n$ . Quite

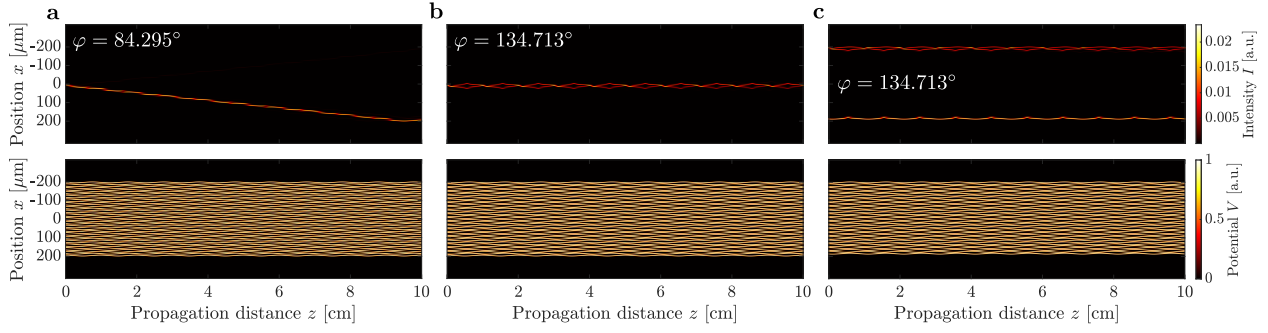


**Fig. 6. Dynamic localization in out-of-phase  $x$ -modulated 1D waveguide arrays** We show the intensity evolution of dynamically localized single-site excitations. The modulation phases  $\varphi_n$  are chosen to alternate between 0 and  $\varphi$  ( $a = 10 \mu\text{m}$ ,  $\omega = 2\pi/cm$ ,  $R = 2.5 \mu\text{m}$ ). In order to achieve dynamic localization we choose  $\varphi$  such that the effective coupling between adjacent waveguides is either (a) minimized,  $\varphi = 84.295^\circ$ , obtaining “shifting” dynamic localization, or (b) maximized,  $\varphi = 134.713^\circ$ , yielding standard dynamic localization. (c) With the lattice configured for standard dynamic localization we observe defect-free surface states. The top (bottom) panels show the evolution of the intensity (waveguide potential).

surprisingly, we observe that, after one period, the light does not re-emerge at the initial waveguide  $n$  but at waveguide  $n+2$ , thus traveling across the lattice during propagation. However, it can also be seen clearly that the wavepacket evolves without any significant diffraction. To the best of our knowledge this constitutes a new form of dynamic localization, which one may call “shifting dynamic localization”. It is worth noting that it is possible to control the direction of the shifting localization by choosing either an even or odd injection site. This intriguing behavior can be understood in the following way. Firstly, the interaction between each pair of waveguides after one period can be regarded as a generalized waveguide beamsplitter as seen in Eq. (7). Therefore, the condition of vanishing coupling implies that light entering either waveguide will emerge in the same waveguide at the output. In other words, in this configuration, the effective waveguide beamsplitter is fully transparent. However, the situation is slightly different in a lattice configuration. In our specific case the light couples completely into the opposite waveguide  $n+1$  at roughly half of the modulation period. Coincidentally, at this point of the propagation, the next-nearest-neighbor waveguide is closest and thus the light continues to couple into waveguide  $n+2$  instead of returning to waveguide  $n$ . This consideration leads to the natural question, as to what happens when the generalized beam splitter is fully reflecting rather than transparent? To answer this, we need to find the modulation phase that maximizes the effective coupling. Using Fig. (3-a) we find the maximum at  $\varphi_d = 134.713^\circ$ . In Fig. (6-b) we show the resulting lattice structure and the evolution of the central excitation. Now we clearly observe what is conventionally understood as dynamic localization, since the light returns to its injection site after each period of the modulation. It is worth to appreciate that the waveguide structures shown in Fig. (6-a,b) are hardly distinguishable to the human eye, and yet they feature fundamentally distinct light coupling behaviour.

Another phenomenon, which is closely related to dynamic localization, is the existence of so-called defect-free surface states [33, 34] in modulated lattices. To be precise, when the lattice is configured to exhibit dynamic localization, then light injected into the edge of such a lattice will remain localized on the edge. As we show in Fig. (6-c) we observe exactly this effect in our out-of-phase modulated arrays. The lattice shown here, is identical to the one in Fig. (6-b) except we have removed the right-most waveguide, in order to show that the defect-free surface mode is observable with both types of lattice terminations.

## 6. Summary & Outlook

To summarize, we have shown that the modulation phase readily enables us to manipulate the local artificial gauge field in waveguide lattices. By adjusting the relative modulation phase between adjacent waveguides we are then able to tune the real- and imaginary part of the effective coupling coefficients. As a proof of concept we have demonstrated numerically the possibility to induce Anderson localization by choosing the modulation phases randomly in both 1D- and 2D-lattices. Since such waveguide lattices are straightforward to implement, our studies enable the testing of our fundamental understanding of wave propagation in disordered systems and to simulate other physical systems such as electron propagation in random magnetic fields. Further, we have shown how to obtain dynamic localization effects by tuning the modulation phases in 1D-lattices. Notably, we found “shifting” dynamic localization, which enables the diffraction-free transport of single-site excitations across 1D lattices.

Looking forward, our proposed technique of out-of-phase modulation may be useful in the design of functional optical devices. As an example, the so-called  $\hat{J}_x$ -lattice, which performs the quite useful discrete fractional fourier-

transform [35, 36], requires the coupling coefficients to follow a parabolic distribution. In this specific case, the conventional method, of engineering the distances between waveguides in order to achieve the desired coupled structure, leads to an unfavorable exponential growth in the distances between the waveguides. Our method, however, does not require any change in the lattice vector and a wide range of coupling profiles may be achievable by a judicious choice of the modulation phases. In this way, our method may help to reduce the footprint of optical coupled structures. We believe this to be a promising direction for future studies.

Another interesting avenue for further investigation, would be the possibility to leverage the modulation phase in the design of topological insulator lattices. Artificial gauge fields already play a crucial role in this area of research, most prominently in the case of Floquet topological insulators. For example, the topological Haldane lattice has been implemented via the helical in-phase-modulation of a honeycomb lattice of optical waveguides [16], which induces a transversally-homogeneous artificial gauge field. Instead, with the modulation phase as a new degree of freedom, is it possible to obtain topological lattices exhibiting transversally-structured artificial gauge fields? We hope that our work will form a stepping stone for research in this exciting direction.

Finally, in this work we have limited the modulation radius to a maximum value in order to avoid waveguide overlap during the modulation. It would be an intriguing possibility to relax this condition and to allow for partial waveguide overlap, complete merging or even crossing of the waveguides. Evidently, then the tight-binding approximation would break down and it is not entirely clear whether an effective Hamiltonian can be properly defined under these conditions. We plan to investigate all these possibilities in future work.

## 7. Backmatter

**Funding.** Deutsche Forschungsgemeinschaft (Project number 255652081)

**Acknowledgments.** The authors acknowledge support by Deutsche Forschungsgemeinschaft (DFG) within the priority program SPP 1839 Tailored Disorder (BU 1107/12-2, PE 2602/2-2). The authors thank Miguel A. Bandres for tremendously insightful discussions and suggestions.

**Disclosures.** The authors declare no conflicts of interest.

**Data Availability Statement.** Data underlying the results presented in this paper are not publicly available at this time but may be obtained from the authors upon reasonable request.

## References

1. P. W. Anderson, "Absence of diffusion in certain random lattices," *Phys. Rev.* **109**, 1492–1505 (1958).
2. F. Evers and A. D. Mirlin, "Anderson transitions," *Rev. Mod. Phys.* **80**, 1355–1417 (2008).
3. A. Lagendijk, B. Van Tiggelen, and D. S. Wiersma, "Fifty years of anderson localization," *Phys. today* **62**, 24–29 (2009).
4. T. Ying, Y. Gu, X. Chen, X. Wang, S. Jin, L. Zhao, W. Zhang, and X. Chen, "Anderson localization of electrons in single crystals:  $\text{Li}_x\text{Fe}_7\text{Se}_8$ ," *Sci. Adv.* **2**, e1501283 (2016).
5. L. Macon, J. P. Desideri, and D. Sornette, "Localization of surface acoustic waves in a one-dimensional quasicrystal," *Phys. Rev. B* **44**, 6755–6772 (1991).
6. J. D. Maynard, "Acoustical analogs of condensed-matter problems," *Rev. modern physics* **73**, 401 (2001).
7. Y. Lahini, A. Avidan, F. Pozzi, M. Sorel, R. Morandotti, D. N. Christodoulides, and Y. Silberberg, "Anderson localization and nonlinearity in one-dimensional disordered photonic lattices," *Phys. Rev. Lett.* **100**, 013906 (2008).
8. L. Martin, G. D. Giuseppe, A. Perez-Leija, R. Keil, F. Dreisow, M. Heinrich, S. Nolte, A. Szameit, A. F. Abouraddy, D. N. Christodoulides, and B. E. A. Saleh, "Anderson localization in optical waveguide arrays with off-diagonal coupling disorder," *Opt. Express* **19**, 13636–13646 (2011).
9. G. Di Giuseppe, L. Martin, A. Perez-Leija, R. Keil, F. Dreisow, S. Nolte, A. Szameit, A. F. Abouraddy, D. N. Christodoulides, and B. E. A. Saleh, "Einstein-podolsky-rosen spatial entanglement in ordered and anderson photonic lattices," *Phys. Rev. Lett.* **110**, 150503 (2013).
10. M. Segev, Y. Silberberg, and D. N. Christodoulides, "Anderson localization of light," *Nat. Photonics* **7**, 197–204 (2013).
11. D. N. Christodoulides, F. Lederer, and Y. Silberberg, "Discretizing light behaviour in linear and nonlinear waveguide lattices," *Nature* **424**, 817–823 (2003).
12. W. Bogaerts, P. De Heyn, T. Van Vaerenbergh, K. De Vos, S. Kumar Selvaraja, T. Claes, P. Dumon, P. Bienstman, D. Van Thourhout, and R. Baets, "Silicon microring resonators," *Laser & Photonics Rev.* **6**, 47–73 (2012).
13. S. Walter and F. Marquardt, "Classical dynamical gauge fields in optomechanics," *New J. Phys.* **18**, 113029 (2016).
14. M. Aidelburger, S. Nascimbene, and N. Goldman, "Artificial gauge fields in materials and engineered systems," *Comptes Rendus Physique* **19**, 394–432 (2018).
15. C. Jörg, G. Queralto, M. Kremer, G. Pelegrí, J. Schulz, A. Szameit, G. von Freymann, J. Mompart, and V. Ahufinger, "Artificial gauge field switching using orbital angular momentum modes in optical waveguides," *Light. Sci. & Appl.* **9**, 1–7 (2020).
16. M. C. Rechtsman, J. M. Zeuner, Y. Plotnik, Y. Lumer, D. Podolsky, F. Dreisow, S. Nolte, M. Segev, and A. Szameit, "Photonic floquet topological insulators," *Nature* **496**, 196–200 (2013).
17. Q. Lin and S. Fan, "Light guiding by effective gauge field for photons," *Phys. Rev. X* **4**, 031031 (2014).
18. R. Umucalilar and I. Carusotto, "Artificial gauge field for photons in coupled cavity arrays," *Phys. Rev. A* **84**, 043804 (2011).
19. M. Schmidt, S. Kessler, V. Peano, O. Painter, and F. Marquardt, "Optomechanical creation of magnetic fields for photons on a lattice," *Optica* **2**, 635–641 (2015).
20. H.-T. Lim, E. Togan, M. Kroner, J. Miguel-Sanchez, and A. Imamoglu, "Electrically tunable artificial gauge potential for polaritons," *Nat. communications* **8**, 1–6 (2017).
21. S. Tseskes, E. Ostrovsky, K. Cohen, B. Gjonaj, N. Lindner, and G. Bartal, "Optical skyrmion lattice in evanescent electromagnetic fields," *Science* **361**, 993–996 (2018).

22. Y. Shen, E. C. Martínez, and C. Rosales-Guzmán, “Generation of optical skyrmions with tunable topological textures,” *ACS Photonics* **9**, 296–303 (2022).
23. N. Westerberg, C. Maitland, D. Faccio, K. Wilson, P. Öhberg, and E. M. Wright, “Synthetic magnetism for photon fluids,” *Phys. Rev. A* **94**, 023805 (2016).
24. S. Longhi, “Effective magnetic fields for photons in waveguide and coupled resonator lattices,” *Opt. letters* **38**, 3570–3573 (2013).
25. K. Fang, Z. Yu, and S. Fan, “Realizing effective magnetic field for photons by controlling the phase of dynamic modulation,” *Nat. photonics* **6**, 782–787 (2012).
26. D. H. Dunlap and V. M. Kenkre, “Dynamic localization of a charged particle moving under the influence of an electric field,” *Phys. Rev. B* **34**, 3625–3633 (1986).
27. S. Longhi, M. Marangoni, M. Lobino, R. Ramponi, P. Laporta, E. Cianci, and V. Foglietti, “Observation of dynamic localization in periodically curved waveguide arrays,” *Phys. Rev. Lett.* **96**, 243901 (2006).
28. A. Kiselev, “Localized light waves: Paraxial and exact solutions of the wave equation (a review),” *Opt. Spectrosc.* **102**, 603–622 (2007).
29. J. M. Luttinger, “The effect of a magnetic field on electrons in a periodic potential,” *Phys. Rev.* **84**, 814–817 (1951).
30. A. Eckardt and E. Anisimovas, “High-frequency approximation for periodically driven quantum systems from a floquet-space perspective,” *New J. Phys.* **17**, 093039 (2015).
31. D. Guzman-Silva, M. Heinrich, T. Biesenthal, Y. V. Kartashov, and A. Szameit, “Experimental study of the interplay between dynamic localization and anderson localization,” *Opt. Lett.* **45**, 415–418 (2020).
32. C. Huang, X. Shi, F. Ye, Y. V. Kartashov, X. Chen, and L. Torner, “Tunneling inhibition for subwavelength light,” *Opt. Lett.* **38**, 2846–2849 (2013).
33. I. L. Garanovich, A. A. Sukhorukov, and Y. S. Kivshar, “Defect-free surface states in modulated photonic lattices,” *Phys. Rev. Lett.* **100**, 203904 (2008).
34. A. Szameit, I. L. Garanovich, M. Heinrich, A. A. Sukhorukov, F. Dreisow, T. Pertsch, S. Nolte, A. Tünnermann, and Y. S. Kivshar, “Observation of defect-free surface modes in optical waveguide arrays,” *Phys. Rev. Lett.* **101**, 203902 (2008).
35. S. Weimann, A. Perez-Leija, M. Lebugle, R. Keil, M. Tichy, M. Gräfe, R. Heilmann, S. Nolte, H. Moya-Cessa, G. Weihs, D. N. Christodoulides, and A. Szameit, “Implementation of quantum and classical discrete fractional fourier transforms,” *Nat. Commun.* **7**, 11027 (2016).
36. K. Tschernig, R. de J. León-Montiel, O. S. M. na Loaiza, A. Szameit, K. Busch, and A. Perez-Leija, “Multiphoton discrete fractional fourier dynamics in waveguide beam splitters,” *J. Opt. Soc. Am. B* **35**, 1985–1989 (2018).